Large Stroke Vertical PZT Microactuator With High-Speed Rotational Scanning

Zhen Qiu, Choong-Ho Rhee, Jongsoo Choi, Thomas D. Wang, and Kenn R. Oldham, *Member, IEEE*

***Abstract*— A thin-film piezoelectric microactuator using a novel combination of active vertical translational scanning and passive resonant rotational scanning is presented. Thin-film lead-zirconate-titanate unimorph bending beams surrounding a central platform provide nearly 200-μm displacement at 18 V with bandwidth greater than 200 Hz. Inside the platform, a mirror mount, or mirror surface, supported by silicon dioxide spring beams can be excited to resonance by low-voltage; high-frequency excitation of the outer PZT beams. Over ±5.5° mechanical resonance is obtained at 3.8 kHz and ±2 V. The combination of large translational vertical displacements and high-speed rotational scanning is intended to support real-time cross-sectional imaging in a dual axes confocal endomicroscope. [2013-0351]**

***Index Terms*— Microactuators, piezoelectric transducers, microscopy.**

I. Introduction

A THIN-FILM PIEZOELECTRIC microactuator combining large vertical translation with high-speed, large-angle rotational scanning is presented for performing vertical cross-sectional imaging in a dual axes confocal endomicroscope. In dual axes endomicroscopy, separate off-axis illumination and collection beams are used to perform imaging with high axial resolution (2-5 μm) in biological tissues with large depth of penetration (200-500 μm) [1]. Real-time scanning in the x-z-plane can image the epithelium, where most gastrointestinal tract diseases originate, with the same orientation as tissue sections used by pathologists.

To miniaturize a dual axes confocal architecture to a 5 mm outer diameter instrument for endoscope compatibility (to perform real-time vertical cross-sectional imaging *in vivo*), a dog-bone-shaped micro-mirror must perform both vertical displacement and axial rotation, as in Fig. 1. Vertical displacement for axial, or into-tissue, scanning, should have approximately the same amplitude as the imaging depth, with frequency at least 5 Hz to avoid motion aberrations. Fast-axis lateral scanning is typically achieved with a rotational scanning mirror, with frequencies of 3 to 5 kHz preferred for *in vivo* imaging. For example, 400 μm vertical translation and +/−6° mechanical scanning angle at such speeds gives an 800 × 400 μm field-of-view in tissue in a larger system [1]. While various rotational MEMS scanning mirrors have been demonstrated, they generally lack vertical translation in a single package that would best support cross-sectional imaging instrument size reduction. The few vertical/rotational scanning stages or mirrors reported, shown in Table I, include electrothermal, piezoelectric, and electrostatic designs. These designs that rely on active force in all axes either cannot attain the needed combination of vertical stroke and speed or have lateral scanning frequencies too low for *in vivo* imaging. A dual axes endomicroscope using a commercial DC motor for axial motion has been tested, but the motor is large and has low speed and accuracy due to large inertias and backlash [2].

The scanning actuator presented here, shown in Fig. 2, uses the resonance of an inner rotational scanning mirror to perform high-frequency excitation with a large stroke, thin-film piezoelectric vertical actuator, via a gimbal that simplifies use in imaging. The large work density of thin-film lead-zirconate-titanate (PZT) after a processing to remove underlying silicon enables large vertical translation. Meanwhile, mirror flexures are designed to have high natural frequency for raster scanning while the vertical axis translates. Large translational (nearly 200 μm at 18 V) and rotational motion (over ±5.5° at 2 V AC excitation) has been achieved.

TABLE I
VERTICAL ROTATIONAL MEMS ACTUATORS

Type	Voltage (V)	Vertical axis Freq. (Hz)	Vertical axis Ampl. (μm)	Rotational axis Freq. (kHz)	Rotational axis Ampl.† (°)
Thermal tip-tilt [5]	8	336*	480	0.5	±30
PZT tip-tilt [6]	2	316	32	0.58	5
Electrostatic [7]	150	NR	10	13.5	±12.5
This device	**18**	**280**	**>190**	**>2.8**	**±5.5**

* Mechanical resonance (thermal time constant slower) † Mechanical scan angle (1/2 optical scan angle)

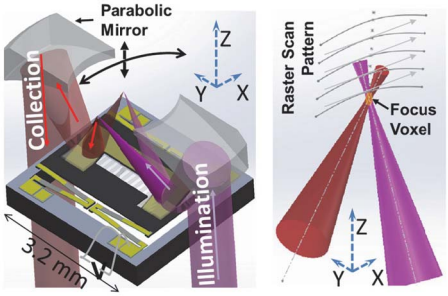

Fig. 1. Desired vertical-rotational stage scanning during cross-sectional dual axes confocal endomicroscope imaging, and detail of raster scanning pattern.

Manuscript received November 12, 2013; revised January 8, 2014; accepted January 19, 2014. Date of publication February 13, 2014; date of current version March 31, 2014. This work was supported in part by the U.S. National Institutes of Health under Grant NIH R01 CA142750, in part by the Army Research Laboratory, and in part by Radiant Technologies, Inc. Subject Editor R. T. Howe.

Z. Qiu is with the Department of Biomedical Engineering, University of Michigan, Ann Arbor, MI 48109 USA (e-mail: zqiu@umich.edu).

C.-H. Rhee, J. Choi, and K. R. Oldham are with the Department of Mechanical Engineering, University of Michigan, Ann Arbor, MI 48109 USA (e-mail: chrhee@umich.edu; jongs@umich.edu; oldham@umich.edu).

T. D. Wang is with the Department of Internal Medicine, Biomedical Enginering, and Mechanical Engineering, University of Michigan, Ann Arbor, MI 48109 USA (e-mail: thomaswa@med.umich.edu).

Color versions of one or more of the figures in this letter are available online at http://ieeexplore.ieee.org.

Digital Object Identifier 10.1109/JMEMS.2014.2303643

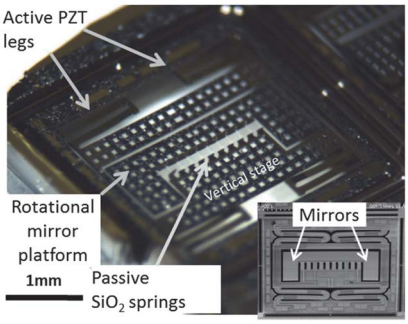

Fig. 2. Vertical-rotational MEMS scanning stage based on active outer vertical displacement and passive inner resonant scanning. Inset: Variant with solid dog-bone mirror surface for dual axes confocal microscopy.

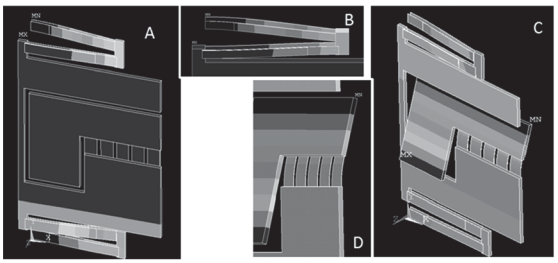

Fig. 3. Finite element model (ANSYS) of vertical-rotational model showing deflection modes during vertical (A, B) and rotational (C, D) motion.

II. Design and Fabrication

The scanning actuator consists of a silicon frame enclosing four outer legs with active thin-film PZT actuation, carrying an inner platform to support a micro-mirror with passive bending beam springs, Fig. 2. The outer legs generate vertical motion using a bend-up/bend-down configuration previously reported in [3]. Each leg consists of two such segments in a folded arrangement, to provide a large range of motion and avoid in-plane rotation of the inner platform.

The inner platform consists of a rectangular gimbal or z-stage surrounding a dog-bone shaped inner mirror or mirror mount. The inner mirror is connected to the gimbal by an array of bending beam flexures. The first bending mode of the flexures, with mirror attached, can be used to generate rotational motion of the mirror, as shown in Fig. 3. In operation, a small, high-frequency excitation of the outer PZT legs is used to excite resonance of the inner mirror and flexure array. This simplifies device design and eliminates the need to include interconnects from the microactuator frame.

The actuator is fabricated by thin-film PZT on encapsulated silicon-on-insulator (SOI) wafer processing as described in [4]. In brief, narrow (3 μm wide) trenches are etched through the device layer of an SOI wafer (30 μm – 2 μm – 500 μm layer thicknesses). These trenches are refilled with low-pressure chemical vapor deposited silicon dioxide, then planarized [Fig. 4(a)]. PECVD SiO_2 is added to augment the base layer to 500 nm after planarization. A bottom Ti/Pt electrode layer (100 nm) is sputtered onto the wafer, after which thin-film PZT (1 μm) is deposited by a chemical solution process. A second Pt electrode (100 nm) is deposited, and then electrode and PZT layers are patterned by ion milling and reactive-ion etching. A gold layer (1 μm) defining bond pads and

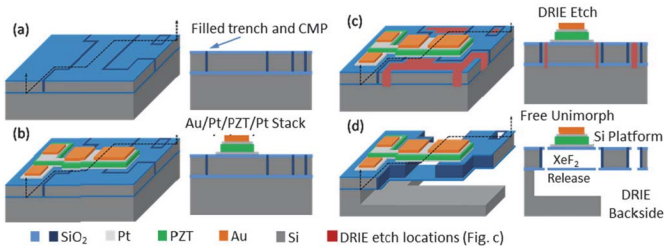

Fig. 4. Actuators are fabricated through (a) deep trench etching and SiO_2 refill to encapsulate rigid silicon structures. (b) Thin-film PZT and metal stack deposition and patterning. (c) Front-side DRIE to separate moving parts. (d) Back-side DRIE and XeF_2 silicon etch to fully rslease PZT unimorphs.

bend-down versus bend-up beam segments is deposited by lift-off [Fig. 4(b)]. Trenches are then etched through the device layer and buried oxide layers into the handle wafer [Fig. 4(c)]. A XeF_2 etch removes device layer silicon from underneath the thin-film PZT, allowing large bending deflections [Fig. 4(d)]. Rigid silicon components of the actuator are protected by the silicon dioxide barrier trenches. When a solid mirror surface is directly included into the actuator, as inset in Fig. 2, a backside DRIE etch may be performed between steps (c) and (d) in Fig. 4 to release a mirror surface formed from the device layer of the SOI wafer.

The passive spring structure in the scanning actuators takes advantage of the two-layer structure of flexible design elements produced by the above fabrication process. A portion of the SOI wafer's buried oxide layer remains present between trenches etched to the handle layer. Under long PZT beams, this oxide layer is observed to buckle and adhere to the underside of the beam. In contrast, stress engineering is performed to break the layer of silicon dioxide on the actuator surface at resonant spring locations, leaving only beams formed from the buried oxide layer. Gold patches deposited on these springs where they join the rigid silicon frame and mirror platform have sufficient residual stress to reliably break the thin surface silicon dioxide layer, leaving only the buried oxide to support the mirror.

This arrangement provides a high quality factor, uniform single layer beam for generating resonant motion. While not as high performance as some other resonator materials, amplitude is limited by air damping and the amplitude of platform oscillation above the resonant frequencies of the active PZT beams. As a result, use of silicon dioxide as a resonator material does not appear to be detrimental to microactuator performance, while permitting direct fabrication compatibility with existing PZT devices.

III. Experimental Testing and Results

Static and dynamic displacement of prototype stages was measured using a He-Ne Laser (Model 1507 Novette™helium-neon laser, JDSU, Milpitas, CA) and a vertical laser displacement sensor (LK-G32, Keyence, Livonia, MI) and PSD (PSM 2-20, OT-301, On-Trak, Irvine, CA). Two types of stage were tested, one with an integrated Au mirror surface, and another with etch holes through the mirror platform, to which a mirror surface could be adhered.

Static platform displacement was measured at multiple points on the gimbal and mirror for leg input voltages from

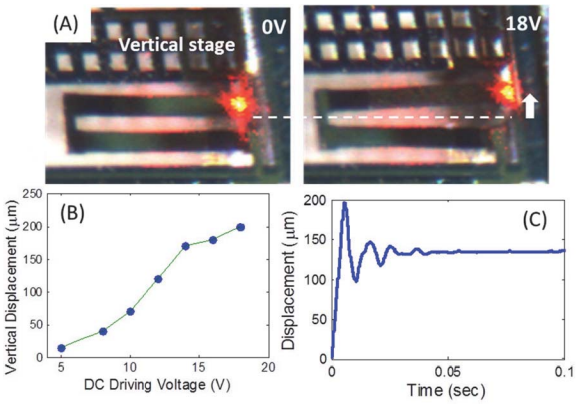

Fig. 5. (A) Optical microscope images of vertical actuator displacement. (B) Displacement versus voltage. (C) Transient response to 10 V step input.

0 to 18 V. A total displacement of 195 μm was obtained, as shown in Fig. 5. The effective electroactive piezoelectric coefficient of thin-film PZT is approximately -80 pC/N, though nonlinearly dependent on voltage. The natural frequency of z-axis translation was measured at 280 Hz. Transient settling time for discrete voltage steps was less than 60 ms. The stage is effectively unidirectional, as most displacement occurs beyond the linear piezoelectric region of the thin-film PZT [8]. Negative DC voltages produce only small negative displacements before returning to upward motion on the opposite side of the piezoelectric butterfly curve, as illustrated by the PZT thin-film characterized in [9].

The inner mirror was excited by a $\pm$2 V sinusoidal input at various DC offset voltages. Resonant motion about the x-axis was observed at 3800 Hz for a mirror platform with etch holes, Fig. 6, and at 2800 Hz for a solid, gold-coated mirror. Peak amplitude was $\pm$5.5° at DC offset of 7 V, with quality factor of about 75, for the mirror with etch holes. These large angular displacements are found to be achievable even in the presence of additional vibration modes occurring at lower frequencies (such as platform rotational modes). Due to large frequency separation, cross-coupling between axes is very small. Disturbance to vertical height from mirror resonance is less than 1 μm. However, non-uniformity of the actuation legs can lead to tilting of the vertical stage, with observed tilting ranging from $<$ 1°to $>$ 2.5°. Passive spring structure softening was observed in both device types, evident in an asymmetric resonant peak and a frequency shift when varying DC offsets. Modeling this nonlinearity is a subject of future work.

The PZT beams act as small capacitive loads of about 2 nF. Power consumption at mirror resonance is on the order of 30 μW. Power needs and thermal self-heating are thus very small. However, the PZT stack is susceptible to displacement due to ambient temperature changes of a few microns.

IV. Discussion and Conclusion

The scanning microactuators described here have achieved $>$195 μm vertical translation and $\pm$5.5° rotation. Range of motion, open-loop vertical axis response time and inner mirror scanning frequencies are fast enough for real-time vertical cross-sectional scanning in a dual axes confocal endomicroscope with a field-of-view of 800 $\times$ 200 μm at a frame rate of $>$5 Hz, based on the performance of previous, handheld imaging systems. Greater vertical displacements may be possible through the use of additional piezoelectric beams, and 3-dimensional imaging may be possible by differential driving of the outer legs. Operation of the piezoelectric scanner is currently constrained by nonlinear effects observed in both slow- and fast-axes. A better understanding of these effects will be required for best image registration with the described devices in endoscopic imaging. Likewise, feedback control may be helpful by using piezoelectric or piezoresistive measurements from the stage to actively regulate vertical and rotational motion. Nonetheless, the large range-of-motion and comparatively high-natural frequencies makes the scanning stage well suited for real-time cross sectional imaging in an endoscopic form factor.

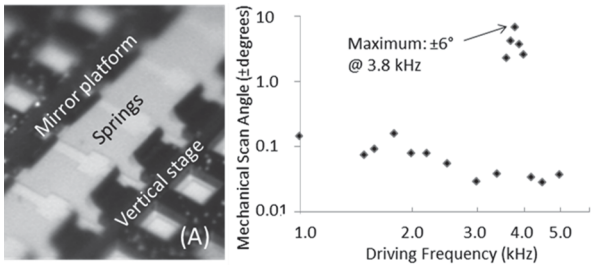

Fig. 6. (A) Optical microscope detail of suspended silicon dioxide spring structure. (B) Mechanical scan angle versus excitation frequency of low-voltage AC excitation to PZT legs.

Acknowledgment

The authors thank the Army Research Laboratory and Radiant Technologies, Inc. for their additional support.

References

[1] Z. Qiu, Z. Liu, X. Duan, B. Joshi, M. Mandella, K. Oldham, *et al.*, "Targeted vertical cross-sectional imaging with handheld near-infrared dual axees confocal fluorescence microscope," *Biomed. Opt. Exp.*, vol. 4, no. 1, pp. 322–330, 2012.

[2] W. Piyawattanametha, H. Ra, Z. Qiu, S. Friedland, J. Liu, E. Garai, *et al.*, "In vivo near-infrared dual-axis confocal microendoscopy in the human lower gastrointestinal tract," *J. Biomed. Opt.*, vol. 17, no. 2, p. 021102, 2012.

[3] Z. Qiu, J. Pulskamp, X. Lin, C.-H. Rhee, T. Wang, R. Polcawich, *et al.*, "Large displacement vertical translational actuator based on piezoelectric thin-films," *J. Micromech. Microsyst. Eng.*, vol. 20, no. 7, p. 075016, 2010.

[4] C. Rhee, J. Pulskamp, R. Polcawich, and K. Oldham, "Multi-degree-of-freedom thin-film PZT actuated micro-robotic leg," *J. Microelectromech. Syst.*, vol. 21, no. 6, pp. 1492–1503, Dec. 2012.

[5] K. Jia, S. Pal, and H. Xie, "An electrothermal tip-tilt-piston microactuator based on folded dual s-shaped bimorphs," *J. Microelectromech. Syst.*, vol. 18, no. 5, pp. 1004–1015, 2009.

[6] Y. Zhu, W. Liu, K. Jia, W. Liao, and H. Xie, "A piezoelectric unimorph actuator based tip-tilt-piston micromirror with high fill factor and small tilt and lateral shift," *Sens. Actuators A, Phys.*, vol. 167, no. 2, pp. 495–501, 2011.

[7] K. Lee, K. Krisnamoorthy, K. Yu, and O. Solgaard, "Single-crystalline silicon micromirrors actuated by self-aligned vertical electrostatic comb drives with piston-motion and rotational capability," *Sens. Actuators A, Phys.*, vol. 114, nos. 2–3, pp. 423–428, 2004.

[8] K. Oldham, J. S. Pulskamp, R. G. Polcawich, and M. Dubey, "Thin-film PZT lateral actautors with extended stroke," *J. Microelectromech. Syst.*, vol. 17, no. 4, pp. 890–899, Aug. 2008.

[9] P. Muralt, A. Kholkin, M. Kohli, and T. Maeder, "Piezoelectric actuation of PZT thin-film diaphragms at static and resonant conditions," *Sens. Actuators A, Phys.*, vol. 53, nos. 1–3, pp. 398–404, 1996.